

## EFFECTS OF CRYSTALS ON THE MECHANICAL PROPERTIES OF $Zr_{52.5}Ti_5Cu_{17.9}Ni_{14.6}Al_{10}$ BULK METALLIC GLASSES

Ferenc SZÉKELY<sup>a</sup>, Elena GILARDI<sup>a</sup>, Simone RAINERI<sup>a</sup>, Silvia SPRIANO<sup>b</sup>, Roberto DOGLIONE<sup>b</sup>,  
Mikhail I. PETRZHIC<sup>c</sup>, Vjacheslav MOLOKANOV<sup>c</sup>, Marcello BARICCO<sup>a</sup>

<sup>a</sup> Dipartimento di Chimica I.F.M. and INFM- Università di Torino, Torino, Italy.

<sup>b</sup> Dipartimento di Ingegneria Chimica e Scienza dei Materiali, Politecnico di Torino, Torino, Italy.

<sup>c</sup> A.A. Baikov Inst. of Metallurgy and Mater. Sci., RAS, Moscow, Russia.

**Abstract** - In this paper the mechanical properties of fully amorphous and partially crystalline  $Zr_{52.5}Ti_5Cu_{17.9}Ni_{14.6}Al_{10}$  alloys were investigated. The changes in hardness and ductility caused by the presence of crystals in the amorphous matrix is presented.

**Resumé** – Effets de cristaux sur les propriétés mécaniques de verres métalliques massifs  $Zr_{52.5}Ti_5Cu_{17.9}Ni_{14.6}Al_{10}$ . Nous avons étudié les propriétés mécaniques d'alliages  $Zr_{52.5}Ti_5Cu_{17.9}Ni_{14.6}Al_{10}$  totalement ou partiellement cristallins. Les changements de dureté et de ductilité causés par la présence de cristaux dans la matrice amorphe sont décrits.

### 1. INTRODUCTION

In certain compositions the glass forming ability of alloys can be very high, meaning that bulk amorphous alloys can be produced by conventional casting methods [1] (i.e. quenching rates of the order of  $10\text{ K}\cdot\text{s}^{-1}$ ). Widely investigated bulk glass forming systems are the Zr-based multicomponent alloys [2-6]. Preparation conditions must be carefully controlled in order to prepare a fully amorphous sample, avoiding the nucleation of crystalline phases during the casting process.

Bulk metallic glasses are interesting for their mechanical properties. A high fracture strength along with a low Young's modulus is promising from the point of view of applications [1,2]. On the other hand amorphous alloys show work softening during plastic deformation, which results in very low plastic elongation. The effect on mechanical properties of crystallites embedded in the amorphous alloys has been investigated by several authors both in the cases of as-cast and annealed samples [2-6]. The presence of large crystals in the as-quenched state usually reduces the fracture strength and the plastic elongation before fracture, while the nanocrystals formed during the crystallization process can improve ductility and strength [2-6].

In this paper the effect of crystals on different mechanical properties in a bulk amorphous alloy of the composition  $Zr_{52.5}Ti_5Cu_{17.9}Ni_{14.6}Al_{10}$  is investigated. The changes of microhardness, compressive deformation and fracture properties are presented in the case of different microstructures.

## 2. EXPERIMENTAL

An arc furnace was used to prepare  $\text{Zr}_{52.5}\text{Ti}_5\text{Cu}_{17.9}\text{Ni}_{14.6}\text{Al}_{10}$  master alloys, starting from elements of high purity. The ingots were re-melted three times to obtain a good homogeneity. Bulk amorphous samples were prepared using jet casting into a copper mould in controlled atmosphere. Structural characterization was performed by X-ray diffraction using  $\text{Cu K}\alpha$  radiation. Microstructure and fracture surfaces were studied by scanning electron microscopy. The amorphous-to-crystalline transformation was followed by DSC, both in continuous heating and under isothermal conditions. Hardness was determined at room temperature with a typical load of 1N. The piling-up behaviour around indentations was characterized by atomic force microscopy (AFM). Compressive tests were performed on machined samples (diameter 2.6 mm, length 5.4 mm) at a strain rate of  $10^{-3} \text{ s}^{-1}$ .

## 3. RESULTS AND DISCUSSION

### 3.1. Synthesis and crystallization

XRD patterns of  $\text{Zr}_{52.5}\text{Ti}_5\text{Cu}_{17.9}\text{Ni}_{14.6}\text{Al}_{10}$  bulk metallic glasses are shown in *figure 1* (left). Depending on preparation conditions, fully amorphous and partially crystalline samples were obtained by copper moulding. The most important factors determining the resulting structure are the quenching rate, the quality of the surface of the mould, and the oxygen concentration. In fact, the presence of oxygen, either from the master alloy or from the atmosphere promotes crystallization through the formation of a cubic  $\text{NiZr}_2$  structure, known as big-cube phase. The formation of big

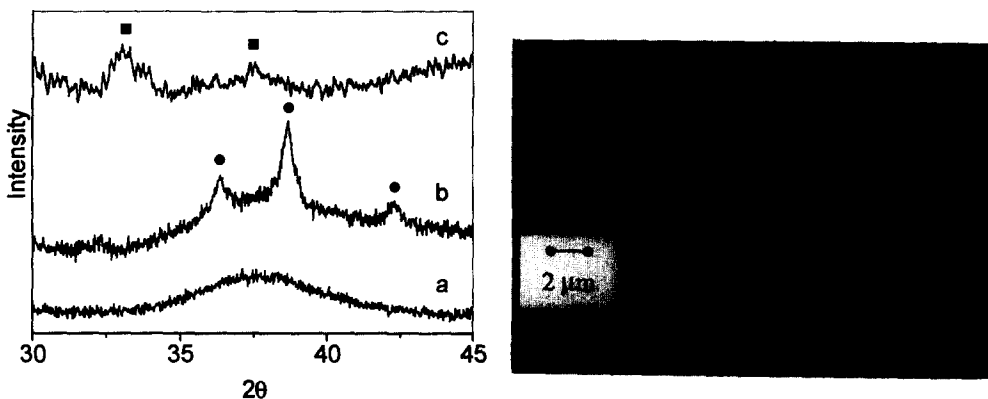


**Figure 1.** Left: X-ray diffraction patterns of fully amorphous (a), partially crystalline (b) and crystallized (c)  $\text{Zr}_{52.5}\text{Ti}_5\text{Cu}_{17.9}\text{Ni}_{14.6}\text{Al}_{10}$  bulk metallic glasses (■  $\text{NiZr}_2$ ; ● big cube). Right: Microstructure of sample (b).

cube phase in the case of the present alloy system was reported also for rapidly quenched ribbons [7]. The big-cube phase can be formed in the presence of oxygen both during casting and during crystallization, resulting in significantly different lattice parameters [7]. The crystals of the big cube phase are homogeneously distributed in the amorphous matrix and have an average size of less than one  $\mu\text{m}$ , as shown in *figure 1* (right).

The crystalline phases formed by crystallization from an originally fully amorphous sample are different, as shown in *figure 1*, curve c. Nanosized  $\text{NiZr}_2$  tetragonal crystals are formed after

annealing at 510°C. At higher temperatures, AlNiZr hexagonal crystals are also found [6].

### 3.2. Effect of crystalline fraction on hardness

It has been reported that the presence of a nanocrystalline phase in the amorphous matrix improves mechanical properties such as hardness [2-6]. So, microhardness measurement was applied to follow the crystallization process both in isothermal conditions and during continuous heating.

In the case of isothermal crystallization, hardness and DSC curves are plotted in *figure 2* (left) as a function of annealing time at 420 °C. The calorimetric curve shows a two step crystallization

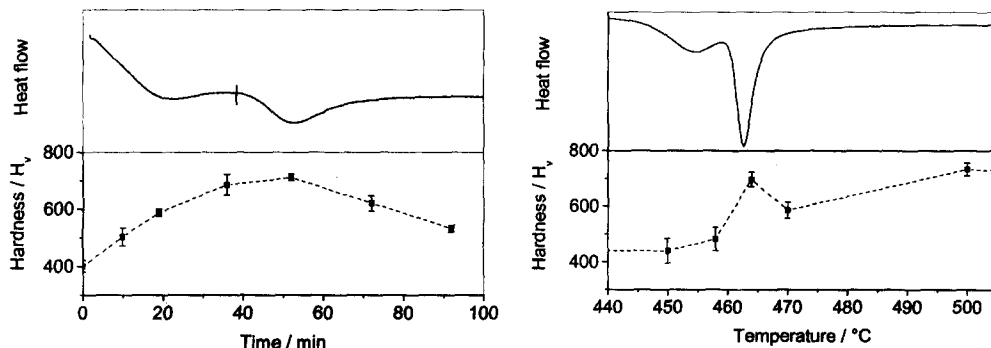


**Figure 2.** DSC trace and hardness change during isothermal heat treatment at 420 °C (left) and continuous heating at 10 K·min<sup>-1</sup> (right) of a fully amorphous  $\text{Zr}_{52.5}\text{Ti}_5\text{Cu}_{17.9}\text{Ni}_{14.6}\text{Al}_{10}$  bulk metallic glass.

process, during which the hardness increases up to the maximum of the second DSC peak, then it decreases. A maximal hardness of 780 HV is reached after 50 min of annealing. The hardness change versus temperature along with the DSC heat flow during continuous heating with heating rate of 10 K·min<sup>-1</sup> is also shown in *figure 2* (right). The hardness increases during the crystallisation process up to the maximum of the second DSC peak then decreases, as in the case of isothermal

treatment. A further increase of the temperature results in an increase of the hardness.

In order to interpret hardness behaviour, one has to take into account two possible hardening effects. Firstly, a hardness enhancing effect may be due to the presence of precipitates [1,2] which are blocking the motion of shear bands. In addition, a hardening effect in the amorphous matrix may be due to a compositional changes during crystallization [8].

In the present case, the crystallization takes place in a two-stage process which suggests a primary mechanism. The decrease of hardness is probably caused by the decreasing volume fraction of the

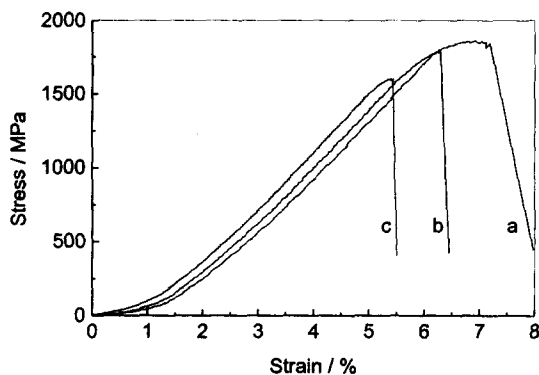


**Figure 3.** Compressive test of  $\text{Zr}_{52.5}\text{Ti}_5\text{Cu}_{17.9}\text{Ni}_{14.6}\text{Al}_{10}$  bulk metallic glasses: fully amorphous (a), and crystallized at 420 °C for 40 minutes (b) and 90 minutes (c).

remaining amorphous matrix.

### 3.3. Compressive deformation and fracture

The deformation behaviours of different samples were investigated by compression tests. The compressive curves of the amorphous alloy, as well as of the one annealed at 420 °C for 40 and 90 minutes are plotted in *figure 3*.

The fully amorphous sample shows a fracture stress of 1860 MPa and an elongation of around 2% and a Young's modulus of 66 GPa. After annealing, the Young's modulus slightly increases. The plastic regime becomes smaller in the presence of crystals, which suggests that the precipitating second phase makes the alloy more brittle.

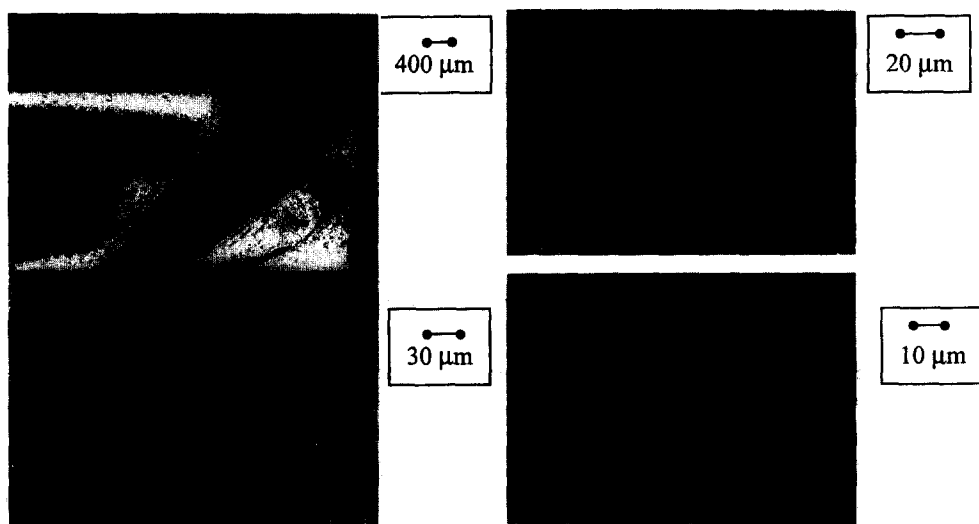


**Figure 4.** Shape of the fractured amorphous sample (left top), fracture surface of the amorphous sample (right top), fracture surface of the sample with quenched-in crystals (left bottom) and fracture surface of nanocrystallized sample (bottom right).

The shape of the fully amorphous sample after fracture in compression test is shown in *figure 4*. The fractured surface is inclined to the load axis at an angle of 45 degrees. This suggests that the fracture is localized along the slip bands formed during deformation. The fracture surface of the totally amorphous sample (*figure 4*) consists mainly of well developed vein patterns and shear bands, clearly indicating ductile fracture. The fracture surface of a partially crystallized sample is also shown in *figure 4*. It shows structural features like the fully amorphous alloy, i.e. vein patterns and shear bands, but signs of brittle fracture can also be seen.

The partially crystalline alloy formed during casting contains more and larger crystallites than the partially crystallized alloy. The fracture surface of this alloy (*figure 4*) indicates the presence of brittle fracture, although there are still some traces vein patterns due to a ductile fracture.

From compression tests and fracture surface analysis one can conclude that the presence of crystallites embedded in the amorphous matrix increases the brittleness of the alloy. In order to further support this, the fracture toughness was estimated from microhardness tests, by measuring the crack length around the indentation. These measurements were not applicable in the case of fully amorphous alloys since, with the applied force, no cracks were formed. For the partially crystalline alloy, this method gives a fracture toughness value ( $K_{IC}$ ) of 0.2-0.3 MPa·m<sup>1/2</sup>. In the case

of fully amorphous alloys with similar compositions, standard fracture toughness methods give a  $K_{IC}$  value of 100–300  $\text{MPa}\cdot\text{m}^{1/2}$  [9]. This finding also supports the observation that the presence of crystals making the amorphous alloy more brittle. Inoue presented data on a similar composition, which suggest that nanocrystals in the amorphous matrix can significantly increase the fracture toughness, i.e. the ductility [1]. On the contrary, Gilbert et al. [10] published similar results as in the present paper, reporting that the presence of crystals causes the transition to brittle fracture. Similar controversial results have been reported for elongation in compression tests. In fact, for  $\text{Zr}_{53}\text{Ti}_5\text{Cu}_{20}\text{Ni}_{10}\text{Al}_{12}$  bulk metallic glasses, the presence of nanocrystals gives an improvement of elongation from 1.4% for a fully amorphous alloy up to 2.5% for a partially crystallized one [11]. On the contrary, for the  $\text{Zr}_{57}\text{Ti}_5\text{Cu}_{20}\text{Ni}_8\text{Al}_{10}$  bulk metallic glass, nanocrystallization gives a strong reduction of elongation [12].

The fracture mechanics of amorphous alloys have been widely studied in recent years [1, 5, 10, 13]. The fracture proceeds along shear bands, where work softening takes place. As a consequence, entanglement of shear bands may also improve ductility [13]. The nucleation of shear bands during compression may be promoted by the deformation field generated by nanocrystal formation. So, ductility of partially crystallized samples is expected to be strongly related to the size and distribution of nanocrystals.

The presence of crystals of the big cube phase in any case leads to the embrittlement of the alloy, because fracture is dominated by the crystalline behaviour [14].

### 3.4. Indentation profile measurements

In the case of an indentation measurement, the material can form pile-ups or sink-ins around the indentation, depending on the plastic behaviour of the material. Recently it has been shown [15] that a connection exists between the shape of the pile-up and the hardening exponent  $n$  of  $\sigma \propto \varepsilon^n$ , measured during tensile tests.

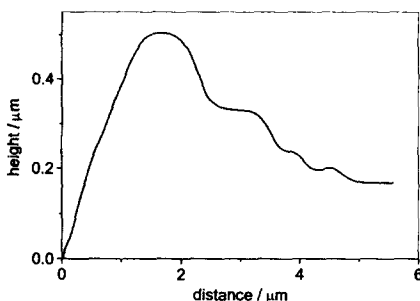
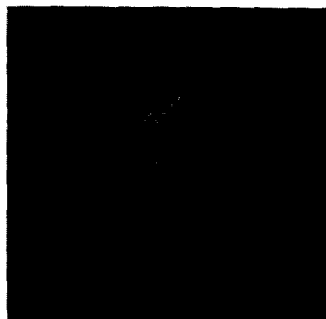


**Figure 5.** Left: AFM image of the piled-up material around Vickers indentation in fully amorphous  $\text{Zr}_{52.5}\text{Ti}_5\text{Cu}_{17.9}\text{Ni}_{14.6}\text{Al}_{10}$  bulk metallic glass. Right: Height profile of indentation.

A typical AFM image of pile-up of the material after Vickers indentation in the fully amorphous alloy is shown in figure 5 along with the height profile of the material. Using the results of Alcalá et al. [15] this corresponds

to a hardening exponent  $n$  of 0.17. However, in the case of amorphous alloys, at least in the case of uniaxial deformation, usually no hardening effects are reported. The observed hardening in the present experiment can be explained considering that Vickers indentation does not give uniaxial load. In this case, slip bands can be entangled, causing hardening. In the case of cold rolling, an increase in strength was observed in a  $\text{Zr}_{55}\text{Cu}_{33}\text{Ni}_5\text{Al}_{10}$  bulk metallic glass [13], which may be also related to work hardening effects.

It has been recently observed that during indentation in BMGs of the present composition, nanocrystals can nucleate near the shear bands, giving a microstructure similar to that observed

after heat treatment [16]. So nanocrystals formed during deformation may affect mechanical properties similarly to those formed during crystallization.

**Acknowledgments:** Work performed for RTN/BMG project (HPRN-CT-2000-00033). Serena Bertarione is acknowledged for AFM analysis.

#### 4. REFERENCES

- [1] A. Inoue, Stabilization of metallic supercooled liquid and bulk amorphous alloys, *Acta mater.*, 48 (2000) 279–306.
- [2] A. Inoue, Mechanical properties of Zr-based bulk glassy alloys containing nanoscale compound particles, *Intermetallics*, 8 (2000) 455–468.
- [3] A. Leonhard, L. Xing, M. Heilmaier, A. Gebert, J. Eckert, L. Schultz, Effect of crystalline precipitations on the mechanical behaviour of bulk glass forming Zr-based alloys, *NanoStruct. Mat.*, 10 (1998) 805–817.
- [4] M. Baricco, A. Castellerio, S. Raineri, S. Spriano, R. Doglione, M. Petrzlik, V. Molokanov, Effect of crystallisation on mechanical properties of a  $Zr_{52.5}Ti_5Cu_{17.9}Ni_{14.6}Al_{10}$  bulk metallic glass, in *Proceedings of 22<sup>nd</sup> Int. Symp. on Mater. Sci.*, edited by A. Dinesen, M. Eldrup, D. J. Jensen, S. Linderroth, T. Pedersen, N. Pryds, A. Pedersen, J. Wert, Risø Nat. Lab, Roskilde, Denmark (2001) 199–204.
- [5] Z. Bian, G. Chen, G. He, X. Hui, Microstructure and ductile-brittle transition of as-cast Zr-based bulk glass alloys under compressive testing, *Mater. Sci. Eng., A* 316 (2001) 135–144.
- [6] J. Wang, B. Choi, T. Nieh, C. Liu, Crystallization and nanoindentation behavior of a bulk Zr-Al-Ti-Cu-Ni amorphous alloy, *J. Mater. Res.*, 15 (2000) 798–806.
- [7] M. Baricco, S. Spriano, I. Chang, M. Petrzlik, L. Batezzati, Big cube phase formation in Zr-based metallic glasses, *Mater. Sci. Eng., A* 304–306 (2001) 305–310.
- [8] A.L. Greer, Partially or fully devitrified alloys for mechanical properties, *Mater. Sci. Eng. A*, 304–306 (2001) 68–72.
- [9] P. Lowhaphandu, J. Lewandowski, Fracture toughness and notched toughness of bulk amorphous alloy: Zr-Ti-Ni-Cu-Be, *Scripta Mater.*, 38 (1998) 1811–1817.
- [10] C. Gilbert, V. Schroeder, R. Ritchie, Mechanism for fracture and fatigue-crack propagation in a bulk metallic glass, *Metall. Mater. Trans.*, 30A (1999) 1739.
- [11] C. Fan, A. Inoue, Ti-containing Zr based bulk amorphous/nanocrystalline composite alloys, *Mater. Trans. JIM*, 41 (2000) 1467–1470.
- [12] L. Xing, C. Bertrand, J.-P. Dallas, M. Cornet, Nanocrystal evolution in bulk amorphous  $Zr_{57}Cu_{20}Al_{10}Ni_8Ti_5$  alloy and its mechanical properties, *Mater. Sci. Eng., A* 241 (1998) 216–225.
- [13] Y. Yokoyama, K. Yamano, K. Fukaura, H. Sunada, A. Inoue, Enhancement of ductility and plasticity of  $Zr_{55}Cu_{30}Al_{10}Ni_5$  bulk glassy alloy by cold rolling, *Mater. Trans. JIM*, 42 (2001) 623–632.
- [14] G. He, J. Lu, Z. Bian, D. Chen, G. Chen, G. Tu, G. Chen, Fracture morphology and quenched-in precipitates induced embrittlement in a Zr-based bulk glass, *Mater. Trans. JIM*, 42 (2001) 356–364.
- [15] J. Alcalá, A. Barone, M. Anglada, The influence of plastic hardening on surface deformation modes around Vickers and spherical indents, *Acta Mater.*, 48 (2000) 3451–3464.
- [16] J.-J. Kim, Y. Choi, S. Suresh, A. Argon, Nanocrystallization during nanoindentation of a bulk amorphous metal alloy at room temperature, *Science*, 295 (2002) 654–657.